

Nucleon sea in the effective chiral quark model

Yong Ding and Rong-Guang Xu

Department of Physics, Peking University, Beijing 100871, China

Bo-Qiang Ma*

CCAST (World Laboratory), P.O. Box 8730, Beijing 100080, China

Department of Physics, Peking University, Beijing 100871, China[†]

Abstract

The asymmetries of both light-flavor antiquark $\bar{d}(x) - \bar{u}(x)$ and strange-antistrange $s(x) - \bar{s}(x)$ distributions of the nucleon sea are considered with more details in the effective chiral quark model. We find that the asymmetric distribution of light-flavor antiquarks $\bar{d}(x) - \bar{u}(x)$ matches the experiment data well and that the asymmetry of strange and antistrange distributions can bring about 60-100% correction to the NuTeV anomaly of $\sin^2 \theta_w$, which are three standard deviations from the world average value measured in other electroweak processes. The results on the correction to the NuTeV anomaly are insensitive to the inputs of the constituent quark distributions and the cut-off parameters. The ratios of $\bar{d}(x)/\bar{u}(x)$ and $s(x)/\bar{s}(x)$ are also discussed, and it is found that the ratio $s(x)/\bar{s}(x)$ is compatible with the available experiments with an additional symmetric sea contribution being considered effectively.

PACS numbers: 12.39.Fe, 11.30.Fs, 13.15.+g, 13.60.Hb

[†] Mailing address.

*Electronic address: mabq@phy.pku.edu.cn; corresponding author.

I. INTRODUCTION

The physics community has been puzzled since the NuTeV Collaboration reported the anomaly that the value: $\sin^2 \theta_w = 0.2277 \pm 0.0013$ (stat) ± 0.0009 (syst), which was measured in deep inelastic scattering (DIS) of (anti-)neutrino from the nuclear target with possible uncertainties and errors having been considered [1], is deviated from the standard model (SM). The Weinberg angle (or weak angle) θ_w is one of the important quantities in the electroweak theory, and can be determined from various experimental methods, such as atomic parity violation, W and Z masses, elastic and inelastic neutrino scattering, and so on. At present, the world accepted value is $\sin^2 \theta_w = 0.2227 \pm 0.0004$. The NuTeV Collaboration measured the value of $\sin^2 \theta_w$ by using the ratio of (anti-)neutrino neutral-current to charged-current cross sections on iron [1], which is closely related to the Paschos-Wolfenstein (P-W) relation [2]:

$$R^- = \frac{\sigma_{NC}^{\nu N} - \sigma_{NC}^{\bar{\nu} N}}{\sigma_{CC}^{\nu N} - \sigma_{CC}^{\bar{\nu} N}} = \frac{1}{2} - \sin^2 \theta_w. \quad (1)$$

The validity of this relation is based on the fundamental assumptions of isoscalar target, charge symmetry and strange symmetry $s(x) = \bar{s}(x)$, which give rise to a large number of theoretical and experimental investigations on this issue. Possible sources of the NuTeV anomaly beyond the SM have been discussed [3]. However, before speculating on the possible new physics, one should first check carefully the *standard* effect and the theoretical uncertainties within quantum chromodynamics (QCD).

Here, we make a broad review of the main mechanisms which have been used to investigate the NuTeV anomaly. The P-W relation holds for a nuclear target provided that the nucleus is in the isoscalar state, which means that various strong interaction effects must cancel out in the ratio. But the actual targets used in the neutrino experiments are usually non-isoscalar nuclei with a significant neutron excess, such as the iron target in the NuTeV experiment. Kumano [4] investigated a conventional explanation in terms of a nuclear modification caused by the difference between the u - and d -valence distributions when the charge and baryon-number conservation for nuclei are considered. He and his collaborators estimated this effect to the NuTeV $\sin^2 \theta_w$ value by using a χ^2 analysis method to reproduce nuclear data on the structure function F_2 and the cross-section of Drell-Yan processes, and noticed that the effect is not large enough to explain the whole NuTeV anomaly in their later work [5]. And Kulagin [6] not only took into account the neutron excess correction to the P-W relation for a neutron-rich target, but also discussed other corrections to the P-W relation caused

by other nuclear effects: the Fermi motion, nuclear binding, nuclear shadowing, etc. In addition, nuclear effects were completely estimated and the shift to the NuTeV anomaly was given with some uncertainties in Ref. [7] by using a particular nuclear x -rescaling model to describe the structure functions in (anti-)neutrino-nucleus DIS. Also, there are other suggestions [8] from a conservative point of views.

Another fundamental assumption is charge symmetry which is a more restricted form of isospin invariance involving a rotation of 180° about the “2” axis in isospin space, or more specifically, the isospin symmetry for the $u \leftrightarrow d$ exchanges between protons and neutrons [9]. However, there have been some discussions about the correction to the P-W relation due to this symmetry breaking. Sather [10] first pointed out that the charge symmetry violation (CSV) should largely affect the extraction of $\sin^2 \theta_w$ from the neutrino collision and gave an estimation about it. The similar result was given in Ref. [11] that CSV effect should reduce about one-third of the discrepancy between the NuTeV result and the accepted average value of $\sin^2 \theta_w$. On the contrary, Cao and Signal [12] calculated the nonperturbative effect of CSV within the meson cloud model framework and showed no contribution to the NuTeV anomaly. At this stage, we still have no direct experimental evidences to point to a substantial violation of CS in parton distributions. Only there are some up limits in experiment for the CSV, because the effect of CSV usually confuses with the asymmetry of s and \bar{s} distributions.

The asymmetry of strange and antistrange quark distributions may imply an additional source for the anomaly. The topic of strange content in the nucleon sea is one of the most challenging issues in the hadron physics, especially for its connection to the proton spin problem and to the NuTeV anomaly. For the part of nucleon sea generated through gluon splitting $g \rightarrow q\bar{q}$ in perturbative QCD, CP symmetry is expected in the quark and antiquark distributions in the leading order. It has been argued recently that there is a strange-antistrange asymmetry in perturbative QCD at three-loop [13], however, the perturbative QCD alone definitely predicts a non-vanishing and Q -dependent value of strange-antistrange asymmetry which would have a very small contribution to the extraction of $\sin^2 \theta_w$. So the cause of a sizable asymmetry of the nucleon strange sea should be of nonperturbative origin [14, 15, 16]. Furthermore, it is highly probable that the momentum distributions of strange and antistrange are different in the nucleon sea, although the total number of strange quark and antiquark occurring as quantum fluctuations must be precisely equal

to conserve the strangeness quantum number. The consequence on the NuTeV anomaly from possible asymmetry of strange and antistrange quark distributions in the nucleon sea was examined by Cao and Signal [12] utilizing the meson cloud model [15, 17] and the result is fairly small and has no significant effect on the NuTeV result. Oppositely, it was shown [18] that the light-cone baryon-meson fluctuation model proposed by Brodsky and Ma [14] can describe the second moment $S^- \equiv \int_0^1 x[s(x) - \bar{s}(x)]dx$ and produce an asymmetry of $s(x)$ and $\bar{s}(x)$ distributions which could remove roughly 30-80% of the discrepancy between the NuTeV result and other determination of $\sin^2 \theta_w$. Also, in Ref. [19], the asymmetric $s - \bar{s}$ distribution treated in a different framework of non-perturbative hadronic $K + \Lambda$ fluctuations is found to reduce the NuTeV result to only about 2 standard deviations from SM, while the realistic behavior of the strange sea distribution $[xs(x) + x\bar{s}(x)]/2$ is also reasonably reproduced. Kretzer *et al.* [20] obtained QCD correction by calculating the next-to-leading-order (NLO) neutrino cross sections and studied the shift of $\sin^2 \theta_w$ which is closely correlated with $s(x) \neq \bar{s}(x)$ parton distribution function sets and isospin violation with some uncertainties. It is also noticed that the contribution to the NuTeV anomaly changes sign from “-” to “+” when S^- is calculated [21] by using the Lagrange Multiplier method. A more reliable theoretical analysis in the chiral quark model has been given in Ref. [22], in which it is shown that the NuTeV anomaly can be accounted for by at least 60% without sensitivity to the inputs of constituent quark distributions and cut-off parameters. Recently, Wakamatsu [23] gave also a theoretical analysis based on the flavor SU(3) chiral quark soliton model by introducing a parameter of the effective mass difference between strange and nonstrange quarks and predicted a fairly large asymmetry of s - and \bar{s} -quark distributions which would solely resolve the NuTeV anomaly, in similar to the conclusion in Ref. [22]. In addition, Szczurek *et al.* [24] discussed more earlier the dressing of constituent quark with a pseudoscalar meson cloud within the effective chiral quark model by including the effect of SU(3)_f symmetry violation explicitly. They found more pions and kaons in the nucleon than what predicted by traditional meson cloud model and pointed out that the effective chiral quark model may lead to a sizeable asymmetric strangeness content of the nucleon sea.

As we know that the nucleon sea has received attention for a long time because of the abundant phenomena which are away from the naive theoretical expectations. For example, the Gottfried sum rule (GSR) [25] violation is related to the light-flavor antiquark asymmetry

in the nucleon sea and has been measured in several experiments. At the same time, there are some models, such as: the meson cloud model [26, 27] in which the relative success was obtained in both the difference and the ratio of \bar{d} and \bar{u} by including the perturbative component; Pauli blocking effect which first suggested by Field and Feynman [28]; and several different types of chiral models and so on, proposed to explain the violation of Gottfried sum rule. And another case is the proton spin crisis [29] and its connection to the strange content in the nucleon sea [30]. Usually, the distributions of s and \bar{s} are assumed to be symmetric, but this is neither proved theoretically nor experimentally. Moreover, some measurements and analyses [31, 32, 33] show that the distributions of strange and antistrange quark may be asymmetric. A joint fit [34] to the neutrino charged-current cross sections [35] and charged lepton structure function data was made by the CDHS Collaboration and some improvements were achieved in the fits if asymmetry in the strange sea was allowed.

In this paper, we present the more detailed calculation of the asymmetric distributions for both the light-flavor antiquarks $\bar{d}(x)$ and $\bar{u}(x)$ and the strange content in the nucleon sea by using the effective chiral quark model along with our previous work [22], and find that the distributions of $\bar{d}(x) - \bar{u}(x)$, $\bar{d}(x) + \bar{u}(x)$, $x(s(x) + \bar{s}(x))$ and $s(x)/\bar{s}(x)$ match well with the experimental data, when additional symmetric sea contributions being considered effectively by taking into account the difference between model results and data parametrization. Furthermore, it should be pointed out that the asymmetry of $s(x)$ and $\bar{s}(x)$ distributions could remove roughly the NuTeV anomaly by at least 60%, and it is more remarkable that this conclusion is insensitive to the different inputs of the effective chiral quark model.

II. THE SEA CONTENT IN THE EFFECTIVE CHIRAL QUARK MODEL

The effective chiral quark model, established by Weinberg [36], and developed by Manohar and Georgi [37], has been widely accepted by the hadron physics society as an effective theory of QCD at low energy scale. The effective chiral quark model has an apt description of its important degrees of freedom in terms of quarks, gluons and Goldstone (GS) bosons at momentum scales relating to hadron structure. There has been a prevailing impression that the effective chiral quark model is successful in explaining the violation of GSR (which was first detected by the New Muon Collaboration at CERN [38]) by the analysis of Eichten, Hinchliffe and Quigg [39]. Also, this model plays an important role in explaining the proton

spin crisis [29] by Cheng and Li [40]. A recent study by us [22] shows that the strange-antistrange asymmetry within the effective chiral quark model could explain the NuTeV anomaly also. It is the purpose of this paper to provide a more detailed analysis on the strange-antistrange asymmetry and its connection to the light-flavor sea asymmetry in the effective chiral quark model.

The chiral symmetry at high energy scale and its breaking at low energy scale are the basic properties of QCD. Because the effect of the internal gluons is small in the effective chiral quark model at low energy scale, the gluonic degrees of freedom are negligible when comparing to those of the GS bosons and quarks. In this picture, the valence quarks which are contained in the nucleon fluctuate into quarks plus GS bosons, which spontaneously break chiral symmetry, and any low energy hadron properties should include this symmetry violation. The effective interaction Lagrangian is

$$L = \bar{\psi}(iD_\mu + V_\mu)\gamma^\mu\psi + ig_A\bar{\psi}A_\mu\gamma^\mu\gamma_5\psi + \dots, \quad (2)$$

where

$$\psi = \begin{pmatrix} u \\ d \\ s \end{pmatrix} \quad (3)$$

is the quark field and $D_\mu = \partial_\mu + igG_\mu$ is the gauge-covariant derivative of QCD, with G_μ standing for the gluon field, g standing for the strong coupling constant and g_A for the axial-vector coupling constant determined from the axial charge of the nucleon. V_μ and A_μ are the vector and axial-vector currents which are defined by the following forms:

$$\begin{pmatrix} V_\mu \\ A_\mu \end{pmatrix} = \frac{1}{2}(\xi^+\partial_\mu\xi \pm \xi\partial_\mu\xi^+), \quad (4)$$

where $\xi = \exp(i\Pi/f)$, and Π has the form:

$$\Pi \equiv \frac{1}{\sqrt{2}} \begin{pmatrix} \frac{\pi^0}{\sqrt{2}} + \frac{\eta}{\sqrt{6}} & \pi^+ & K^+ \\ \pi^- & -\frac{\pi^0}{\sqrt{2}} + \frac{\eta}{\sqrt{6}} & K^0 \\ K^- & \bar{K}^0 & \frac{-2\eta}{\sqrt{6}} \end{pmatrix}. \quad (5)$$

With the expansion for V_μ and A_μ in powers of Π/f , it gives $V_\mu = 0 + O(\Pi/f)^2$ and $A_\mu = i\partial_\mu\Pi/f + O(\Pi/f)^2$, where the pseudoscalar decay constant is $f \simeq 93$ MeV. So the effective

interaction Lagrangian between GS bosons and quarks in the leading order becomes [39]

$$L_{\Pi q} = -\frac{g_A}{f}\bar{\psi}\partial_\mu\Pi\gamma^\mu\gamma_5\psi. \quad (6)$$

The framework that we use in this paper is based on the time-ordered perturbative theory in the infinite momentum frame (IMF). Because all particles are on-mass-shell in this frame and the factorization of the subprocess is automatic, we neglect all possible off-mass-shell corrections. In this framework, we can express the quark distributions inside a nucleon as a convolution of a constituent quark distribution in a nucleon and the structure functions of a constituent quark. The light-front Fock decompositions of constituent quark wave functions have the following forms

$$|U\rangle = \sqrt{Z}|u_0\rangle + a_\pi|d\pi^+\rangle + \frac{a_\pi}{\sqrt{2}}|u\pi^0\rangle + a_K|sK^+\rangle + \frac{a_\eta}{\sqrt{6}}|u\eta\rangle, \quad (7)$$

$$|D\rangle = \sqrt{Z}|d_0\rangle + a_\pi|u\pi^-\rangle + \frac{a_\pi}{\sqrt{2}}|d\pi^0\rangle + a_K|sK^0\rangle + \frac{a_\eta}{\sqrt{6}}|d\eta\rangle, \quad (8)$$

and the corresponding picture are shown in Fig. 1. Here, Z is the renormalization constant

The figure shows two rows of Feynman diagrams. The top row is labeled 'U' and the bottom row is labeled 'D'. Each row shows a horizontal line representing a constituent quark, which is equal to a sum of four terms. Each term consists of a horizontal line representing a bare constituent quark, with a dashed arc above it representing a Goldstone boson. The vertices are labeled with quark flavors. For the U quark, the terms are: a bare u quark, a u quark with a pi^0 boson, a d quark with a pi^+ boson, an s quark with a K^+ boson, and a u quark with an eta boson. For the D quark, the terms are: a bare d quark, a d quark with a pi^- boson, a d quark with a pi^0 boson, an s quark with a K^0 boson, and a d quark with an eta boson.

FIG. 1: The dressing of the constituent U and D quarks with Goldstone bosons.

for the bare constituent quarks which are massive and denoted by $|u_0\rangle$ and $|d_0\rangle$, and $|a_\alpha|^2$ are the probabilities to find GS bosons in the dressed constituent quark states $|U\rangle$ for an *up* quark and $|D\rangle$ for a *down* quark, where $\alpha = \pi, K, \eta$. In the effective chiral quark model, the fluctuation of a bare constituent quark into a GS boson and a recoil bare constituent quark can be given [41]:

$$q_j(x) = \int_0^1 \frac{dy}{y} P_{j\alpha/i}(y) q_i\left(\frac{x}{y}\right). \quad (9)$$

This process also can be described in Fig. 2(a). In Eq. (9), $P_{j\alpha/i}(y)$ is the splitting function which gives the probability for finding a constituent quark j carrying the light-cone momentum fraction y together with a spectator GS boson α and having the following form:

$$P_{j\alpha/i}(y) = \frac{1}{8\pi^2} \left(\frac{g_A \bar{m}}{f} \right)^2 \int dk_T^2 \frac{(m_j - m_i y)^2 + k_T^2}{y^2 (1-y) [m_i^2 - M_{j\alpha}^2]^2}, \quad (10)$$

where m_i, m_j, m_α are the masses of the i, j -constituent quarks and the pseudoscalar meson α , respectively, $\bar{m} = (m_i + m_j)/2$ is the average mass of the constituent quarks, and $M_{j\alpha}^2$ is the invariant mass square of the final states:

$$M_{j\alpha}^2 = \frac{m_j^2 + k_T^2}{y} + \frac{m_\alpha^2 + k_T^2}{1-y}. \quad (11)$$

In this paper, we also adopt the definition of the moment of splitting function:

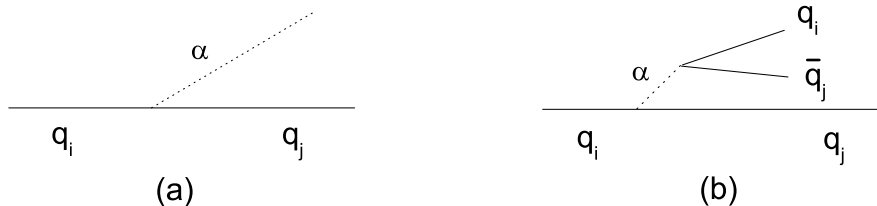


FIG. 2: (a) A constituent quark q_i fluctuates into a Goldstone boson α plus a recoil constituent quark q_j . (b) A Goldstone boson emits a q_i and a \bar{q}_j .

$$\langle x^{n-1} P_{j\alpha/i} \rangle = \int_0^1 x^{n-1} P_{j\alpha/i}(x) dx \quad (12)$$

with the first moment $\langle P_{j\alpha/i} \rangle = \langle P_{\alpha j/i} \rangle \equiv \langle P_\alpha \rangle = |a_\alpha|^2$ [41]. It is conventional that an exponential cutoff is used in IMF calculations because the integral in Eq. (10) requires a momentum cutoff function at the quark-GS boson vertex. Commonly,

$$g_A \rightarrow g'_A \exp \left[\frac{m_i^2 - M_{j\alpha}^2}{4\Lambda^2} \right], \quad (13)$$

with $g'_A = 1$ following the large N_c argument [42], however, $g'_A = 0.75$ was taken in the original work [37]. And Λ is the cutoff parameter, which is determined by the experimental data of the Gottfried sum and the constituent quark mass inputs for the pion. The experimental

value of Gottfried sum is 0.235 ± 0.0026 [38], which is different from the value $1/3$ predicted by the naive parton model in which both the light-flavor sea and the isospin between proton and neutron are SU(2) symmetric [9]. Employing the quark distributions of the effective chiral quark model, we get the Gottfried sum determined by the difference between proton and neutron structure functions:

$$\begin{aligned}
S_{\text{Gottfried}} &= \int_0^1 \frac{dx}{x} [F_2^p(x) - F_2^n(x)] \\
&= \frac{1}{3} \int_0^1 \frac{dx}{x} [u(x) + \bar{u}(x) - d(x) - \bar{d}(x)] \\
&= \frac{1}{3} (Z - \frac{1}{2} \langle P_\pi \rangle + \langle P_K \rangle + \frac{1}{6} \langle P_\eta \rangle) \\
&= \frac{1}{3} (1 - 2 \langle P_\pi \rangle). \tag{14}
\end{aligned}$$

From above equation, we gain the values of Gottfried sum given in table I corresponding to different Λ_π , from which we can find that the appropriate value for Λ_π is 1500 MeV, when the value of Gottfried sum matches well with the experimental data. At the same time, $\langle P_\pi \rangle = 0.149$, $\langle P_K \rangle = 0.085$, $\langle P_\eta \rangle = 0.063$ and $Z = 0.682$. But for K and η mesons, the terms $\langle P_K \rangle$ and $\langle P_\eta \rangle$ in the Gottfried sum cancel out those terms in $Z = 1 - \frac{3}{2} \langle P_\pi \rangle - \langle P_K \rangle - \frac{1}{6} \langle P_\eta \rangle$, so the value of Λ can not be determined from Eq. (14) or experimental data. It is natural to assume that the cutoffs are same for π , K and η mesons in the effective chiral quark model: $\Lambda_\pi = \Lambda_K = 1500$ MeV [24, 41], which is different from the traditional meson cloud model.

TABLE I: The values for Λ and Gottfried sum

Λ_π	1000	1100	1200	1300	1400	1500	1600
Gottfried sum	0.268	0.261	0.253	0.247	0.240	0.234	0.223

When probing the internal structure of GS bosons in Fig. 2(b), we can also write the process in the following form [41]:

$$q_k(x) = \int \frac{dy_1}{y_1} \frac{dy_2}{y_2} V_{k/\alpha}(\frac{x}{y_1}) P_{\alpha j/i}(\frac{y_1}{y_2}) q_i(y_2), \tag{15}$$

where $P_{\alpha j/i}(x) = P_{j\alpha/i}(1-x)$, $V_{k/\alpha}(x)$ is the quark k distribution function in α and satisfies the normalization $\int_0^1 V_{k/\alpha}(x) dx = 1$. Because the mass of η is so high and the coefficient is so small so that the fluctuation of it is suppressed, the contribution is not considered in

our calculation in this paper. From Eqs. (7) and (8), we can have the quark distribution functions of the nucleon by using the splitting function Eq. (10) and the constituent quark distributions u_0 and d_0 which are normalized to 1,

$$\begin{aligned}
u(x) &= Zu_0(x) + P_{u\pi^-/d} \otimes d_0 + V_{u/\pi^+} \otimes P_{\pi^+d/u} \otimes u_0 + \frac{1}{2}P_{u\pi^0/u} \otimes u_0 \\
&\quad + V_{u/K^+} \otimes P_{K^+s/u} \otimes u_0 + \frac{1}{4}V_{u/\pi^0} \otimes (P_{\pi^0u/u} \otimes u_0 + P_{\pi^0d/d} \otimes d_0), \\
d(x) &= Zd_0(x) + P_{d\pi^+/u} \otimes u_0 + V_{d/\pi^-} \otimes P_{\pi^-u/d} \otimes d_0 + \frac{1}{2}P_{d\pi^0/d} \otimes d_0 \\
&\quad + V_{d/K^0} \otimes P_{K^0s/d} \otimes d_0 + \frac{1}{4}V_{d/\pi^0} \otimes (P_{\pi^0u/u} \otimes u_0 + P_{\pi^0d/d} \otimes d_0).
\end{aligned} \tag{16}$$

Here, we define the notation for the convolution integral:

$$P \otimes q = \int_x^1 \frac{dy}{y} P(y)q\left(\frac{x}{y}\right), \tag{17}$$

and

$$V \otimes P \otimes q = \int_x^1 \frac{dy_1}{y_1} \int_{y_1}^1 \frac{dy_2}{y_2} V\left(\frac{x}{y_1}\right)P\left(1 - \frac{y_1}{y_2}\right)q_i(y_2). \tag{18}$$

In the same way, we can have the light-flavor antiquark and strange quark and antiquark distributions:

$$\begin{aligned}
\bar{u}(x) &= V_{\bar{u}/\pi^-} \otimes P_{\pi^-u/d} \otimes d_0 + \frac{1}{4}V_{\bar{u}/\pi^0} \otimes (P_{\pi^0u/u} \otimes u_0 + P_{\pi^0d/d} \otimes d_0), \\
\bar{d}(x) &= V_{\bar{d}/\pi^+} \otimes P_{\pi^+d/u} \otimes u_0 + \frac{1}{4}V_{\bar{d}/\pi^0} \otimes (P_{\pi^0u/u} \otimes u_0 + P_{\pi^0d/d} \otimes d_0), \\
s(x) &= P_{sK^+/u} \otimes u_0 + P_{sK^0/d} \otimes d_0, \\
\bar{s}(x) &= V_{\bar{s}/K^+} \otimes P_{K^+s/u} \otimes u_0 + V_{\bar{s}/K^0} \otimes P_{K^0s/d} \otimes d_0,
\end{aligned} \tag{19}$$

where

$$\begin{aligned}
V_{u/\pi^+} &= V_{\bar{d}/\pi^+} = V_{d/\pi^-} = V_{\bar{u}/\pi^-} \\
&= 2V_{u/\pi^0} = 2V_{\bar{u}/\pi^0} = 2V_{d/\pi^0} = 2V_{\bar{d}/\pi^0} \\
&= \frac{1}{2}V_\pi(x, \mu_{\text{NLO}}^2),
\end{aligned} \tag{20}$$

and

$$V_{\bar{s}/K^+} = V_{\bar{s}/K^0}, V_{u/K^+} = V_{d/K^0}.$$

From above equations, we can reexamine the valence quark distributions $u_v(x) = u(x) - \bar{u}(x)$ and $d_v(x) = d(x) - \bar{d}(x)$ which satisfy the correction normalization with the renormalization constant Z . The parameterizations of parton distributions for mesons are taken from

GRS98 [43] and the sea content in the nucleon is not considered here,

$$V_\pi(x, \mu_{\text{NLO}}^2) = 1.052x^{-0.495}(1 + 0.357\sqrt{x})(1 - x)^{0.365}, \quad (21)$$

$$V_{u/K^+}(x, \mu_{\text{NLO}}^2) = V_{d/K^0}(x, \mu_{\text{NLO}}^2) = 0.540(1 - x)^{0.17}V_\pi(x, \mu_{\text{NLO}}^2), \quad (22)$$

$$V_{\bar{s}/K^+}(x, \mu_{\text{NLO}}^2) = V_{\bar{s}/K^0}(x, \mu_{\text{NLO}}^2) = V_\pi(x, \mu_{\text{NLO}}^2) - V_{u/K^+}(x, \mu_{\text{NLO}}^2). \quad (23)$$

Thus, we can calculate the asymmetries of light-flavor antiquark distributions $\bar{d}(x) - \bar{u}(x)$ and strange-antistrange quark distributions $S^- \equiv \int_0^1 x[s(x) - \bar{s}(x)]dx$ within the effective chiral quark model. In this present work, we choose $m_u = m_d = 330$ MeV, $m_s = 480$ MeV, $m_{\pi^\pm} = m_{\pi^0} = 140$ MeV and $m_{K^+} = m_{K^0} = 495$ MeV. Constituent quark (CQ) model distributions [44] and CTEQ6 parametrization [45] as two different kinds of constituent quark distributions of inputs are adopted. The CQ model distributions have the following forms:

$$\begin{aligned} u_0(x) &= \frac{2}{\text{B}[c_1 + 1, c_1 + c_2 + 2]}x^{c_1}(1 - x)^{c_1 + c_2 + 1}, \\ d_0(x) &= \frac{1}{\text{B}[c_2 + 1, 2c_1 + 2]}x^{c_2}(1 - x)^{2c_1 + 1}, \end{aligned} \quad (24)$$

where $B[i, j]$ is the Euler beta function and $c_1 = 0.65$ and $c_2 = 0.35$ adopted from Ref. [44, 46] are independent of Q^2 with the number and momentum sum rules:

$$\begin{aligned} \int_0^1 u_0(x)dx &= 2, & \int_0^1 d_0(x)dx &= 1, \\ \int_0^1 xu_0(x)dx &+ \int_0^1 xd_0(x)dx &= 1. \end{aligned} \quad (25)$$

It is pointed out that there are other different values for c_1 and c_2 suggested by Ref. [47]. And the CTEQ6 parameterizations are:

$$\begin{aligned} u_0(x) &= 1.7199x^{-0.4474}(1 - x)^{2.9009}\exp[-2.3502x](1 + \exp[1.6123]x)^{1.5917}, \\ d_0(x) &= 1.4473x^{-0.3840}(1 - x)^{4.9670}\exp[-0.8408x](1 + \exp[0.4031]x)^{3.0000}. \end{aligned} \quad (26)$$

As is well-known, the quark distributions measured by experiments at certain Q^2 include not only non-perturbative intrinsic sea but also perturbative extrinsic sea [14]. The intrinsic sea quarks are relatively Q^2 independently (or less dependently) multi-connected with the

valence quarks in the nucleon, but the extrinsic ones are generated mainly from the gluon splitting. Because the correlations between the intrinsic and extrinsic sea quarks are less Q^2 dependent, we give the distribution of $\bar{d}(x) - \bar{u}(x)$ at low energy compared with the experimental ones at high scale shown in Fig. 3. From the figure, we find that the calculated results using the effective chiral quark model match the experiments well with two different sets (CQ model and CTEQ parametrization) of inputs for the constituent quark distributions. The difference between the results from two different inputs may reflect some uncertainties due to the evolution effect which should not cause a big influence on the conclusion. Besides that, we also calculate the strange sea distributions of $x(s(x) + \bar{s}(x))$ and $x(s(x) - \bar{s}(x))$ within this mechanism. For the distributions of $x(s(x) + \bar{s}(x))$, we give the comparison of the results from the effective chiral quark model calculations (with two different sets of inputs) and the NuTeV data parametrization [50] obtained from the LO fits to the dimuon production cross section in $\nu_\mu\text{Fe}$ and $\bar{\nu}_\mu\text{Fe}$ deep inelastic scattering in Fig. 4. From the figure, we can find that the results of the effective chiral quark model calculations are lower than the parametrization of NuTeV data at arbitrary x , which may be caused by the non-considered symmetric strange sea content which will be discussed in Sec. IV

In the effective chiral quark model, it should not be the same for the momentum of strange quark (s) coming from the recoil constituent quark and that of anti-strange quark (\bar{s}) originating from the virtual GS bosons K . Using Eqs. (16) and (19), we can obtain the distributions for $x\delta_s(x)$ shown in Fig. 5 with $\delta_s(x) = s(x) - \bar{s}(x)$. From the figure, we can see that the magnitudes of $x\delta_s(x)$ with CQ model as input are almost twice larger than those with CTEQ parametrization as input, however, the contributions to the NuTeV anomaly, which will be shown in the next section, are similar.

III. APPLICATION TO THE NUTEV ANOMALY

In 1973, Paschos and Wolfenstein [2] suggested to consider the observable Eq. (1) by measuring the ratio of neutral-current to charged-current cross sections for neutrino and antineutrino on isoscalar target to reduce the uncertainties from the productions of the heavy flavor quarks. In Eq. (1), $\sigma_{NC}^{\nu N}$ ($\sigma_{NC}^{\bar{\nu} N}$) is the integral of neutral-current inclusive differential cross section for neutrino (antineutrino) over x and y , and the same to $\sigma_{CC}^{\nu N}$ ($\sigma_{CC}^{\bar{\nu} N}$). The NuTeV Collaboration was inspired by the P-W relation to measure the Weinberg angle

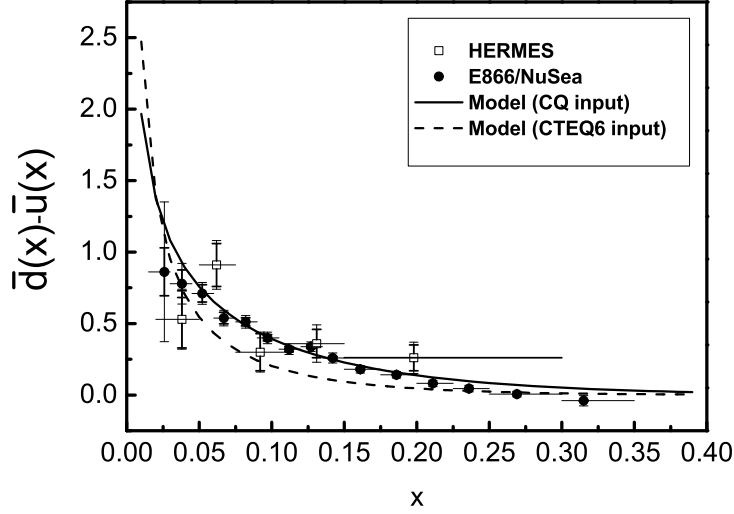


FIG. 3: Distributions for $\bar{d}(x) - \bar{u}(x)$ for $\Lambda_\pi = 1500$ MeV. The solid and dashed curves are the model calculation results in the effective chiral quark model with the constituent quark (CQ) model and the CTEQ6 parametrization as inputs for $u_0(x)$ and $d_0(x)$, respectively. The data are from HERMES ($Q^2 = 2.3$ GeV²) [48] and E866/NuSea ($Q^2 = 54$ GeV²) experiments [49].

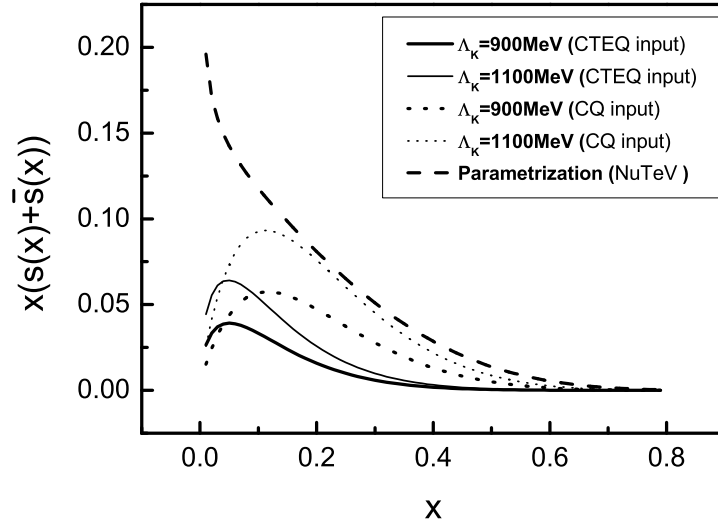


FIG. 4: Distributions for $x(s(x) + \bar{s}(x))$. The solid (dotted) curves are the calculated results in the effective chiral quark model with the CTEQ6 parametrization (CQ model) as input. The thick solid (dotted) curves are for $\Lambda_K = 900$ MeV and the thin ones are for $\Lambda_K = 1100$ MeV, respectively. The dashed curve is for the parametrization of NuTeV data [50].

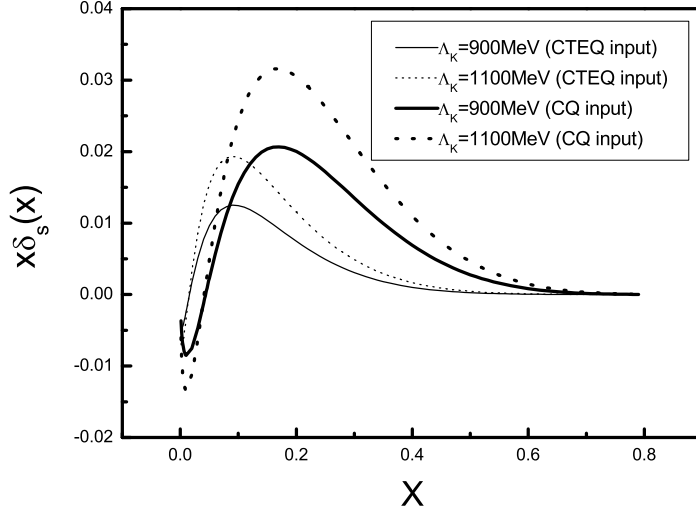


FIG. 5: Distributions of $x\delta_s(x)$ with $\delta_s(x)=s(x) - \bar{s}(x)$ in the effective chiral quark model, when the inputs for $u_0(x)$ and $d_0(x)$ are both constituent quark (CQ) model (thick curves) and CTEQ6 parametrization (thin curves) with $\Lambda_K = 900$ MeV (solid curves) and 1100 MeV (dotted curves).

$\sin^2 \theta_w$ using high statistics separated neutrino and antineutrino beams which arise from π and K mesons decay following the interaction of 800 GeV protons at FNAL. Because the charged-current events contain a final muon that penetrates substantially farther than the hadron shower, neutral- and charged-current events are distinguished by the event length in the counter. The resulting interaction events must be deposited between 20 GeV and 180 GeV in the calorimeter and will be found in the NuTeV detector. The most general form of the differential cross section for neutral-current interactions initiated by (anti-)neutrino on nucleon target is [51]:

$$\begin{aligned} \frac{d^2\sigma_{NC}^{\nu(\bar{\nu})}}{dxdy} = \pi s \left(\frac{\alpha}{2 \sin^2 \theta_w \cos^2 \theta_w M_Z^2} \right)^2 \left(\frac{M_Z^2}{M_Z^2 + Q^2} \right)^2 [xy F_1^Z(x, Q^2) \\ + (1 - y - \frac{xy m_N^2}{s}) F_2^Z(x, Q^2) \pm (y - \frac{y^2}{2}) x F_3^Z(x, Q^2)]. \end{aligned} \quad (27)$$

And similarly, for the (anti-)neutrino-nucleon charged-current reaction, the differential cross section has the form [51]:

$$\begin{aligned} \frac{d^2\sigma_{CC}^{\nu(\bar{\nu})}}{dxdy} = \pi s \left(\frac{\alpha}{2 \sin^2 \theta_w M_W^2} \right)^2 \left(\frac{M_W^2}{M_W^2 + Q^2} \right)^2 [xy F_1^{W^\pm}(x, Q^2) \\ + (1 - y - \frac{xy m_N^2}{s}) F_2^{W^\pm}(x, Q^2) \pm (y - \frac{y^2}{2}) x F_3^{W^\pm}(x, Q^2)], \end{aligned} \quad (28)$$

where M_Z and M_W are the masses of the neutral- and charged-current interacting weak vector bosons, respectively, θ_w is the Weinberg angle, $x = Q^2/2p \cdot q$, $y = p \cdot q/p \cdot k$, and the square of the four momentum transfer for the reaction is $Q^2 = -q^2$, k (p) is the momentum of initial state for neutrino or antineutrino (nucleon) and $s = (k + p)^2$. Besides these, $F_i^{Z(W^\pm)p}(x, Q^2)$ are the structure functions on proton (p), which only depend on x as $Q^2 \rightarrow \infty$, and are written in terms of the parton distributions as [51]

$$\begin{aligned}
\lim_{Q^2 \rightarrow \infty} F_1^{Zp}(x, Q^2) &= \frac{1}{2} \left[((f_V^u)^2 + (f_A^u)^2) (u^p(x) + \bar{u}^p(x) + c^p(x) + \bar{c}^p(x)) \right. \\
&\quad \left. + ((f_V^d)^2 + (f_A^d)^2) (d^p(x) + \bar{d}^p(x) + s^p(x) + \bar{s}^p(x)) \right], \\
\lim_{Q^2 \rightarrow \infty} F_3^{Zp}(x, Q^2) &= 2 [f_V^u f_A^u (u^p(x) - \bar{u}^p(x) + c^p(x) - \bar{c}^p(x)) \\
&\quad + f_V^d f_A^d (d^p(x) - \bar{d}^p(x) + s^p(x) - \bar{s}^p(x))] . \\
F_2^{Zp}(x, Q^2) &= 2x F_1^{Zp}(x, Q^2). \tag{29}
\end{aligned}$$

And the structure functions of charged-current have forms:

$$\begin{aligned}
\lim_{Q^2 \rightarrow \infty} F_1^{W^+p}(x, Q^2) &= d^p(x) + \bar{u}^p(x) + s^p(x) + \bar{c}^p(x), \\
\lim_{Q^2 \rightarrow \infty} F_1^{W^-p}(x, Q^2) &= u^p(x) + \bar{d}^p(x) + \bar{s}^p(x) + c^p(x), \\
\frac{1}{2} \lim_{Q^2 \rightarrow \infty} F_3^{W^+p}(x, Q^2) &= d^p(x) - \bar{u}^p(x) + s^p(x) - \bar{c}^p(x), \\
\frac{1}{2} \lim_{Q^2 \rightarrow \infty} F_3^{W^-p}(x, Q^2) &= u^p(x) - \bar{d}^p(x) - \bar{s}^p(x) + c^p(x), \\
F_2^{W^\pm p}(x, Q^2) &= 2x F_1^{W^\pm p}(x, Q^2). \tag{30}
\end{aligned}$$

One can obtain the structure functions for neutron n by replacing the superscripts $p \rightarrow n$ everywhere in Eqs. (29) and (30). In Eq. (29), f_V^u , f_A^u , f_V^d and f_A^d are vector and axial-vector couplings:

$$\begin{aligned}
f_V^u &= \frac{1}{2} - \frac{4}{3} \sin^2 \theta_w, & f_A^u &= \frac{1}{2}, \\
f_V^d &= -\frac{1}{2} + \frac{2}{3} \sin^2 \theta_w, & f_A^d &= -\frac{1}{2}.
\end{aligned}$$

When the charge symmetry

$$\begin{aligned}
d^n(x) &= u^p(x), \\
u^n(x) &= d^p(x), \\
s^n(x) &= s^p(x) = s(x), \\
c^n(x) &= c^p(x) = c(x), \tag{31}
\end{aligned}$$

and $c(x) = \bar{c}(x)$ are valid, the structure functions for the isoscalar target with the $s(x) \neq \bar{s}(x)$ are given by

$$\begin{aligned}
\lim_{Q^2 \rightarrow \infty} F_1^{W^+N_0}(x, Q^2) &= \frac{1}{2}[d^p(x) + \bar{d}^p(x) + u^p(x) + \bar{u}^p(x) + 2s(x) + 2c(x)], \\
\lim_{Q^2 \rightarrow \infty} F_1^{W^-N_0}(x, Q^2) &= \frac{1}{2}[d^p(x) + \bar{d}^p(x) + u^p(x) + \bar{u}^p(x) + 2\bar{s}(x) + 2c(x)], \\
\lim_{Q^2 \rightarrow \infty} F_3^{W^+N_0}(x, Q^2) &= d^p(x) + u^p(x) - \bar{u}^p(x) - \bar{d}^p(x) + 2s(x) - 2c(x), \\
\lim_{Q^2 \rightarrow \infty} F_3^{W^-N_0}(x, Q^2) &= d^p(x) + u^p(x) - \bar{u}^p(x) - \bar{d}^p(x) - 2\bar{s}(x) + 2c(x), \\
F_2^{W^\pm N_0}(x, Q^2) &= 2xF_1^{W^\pm N_0}(x, Q^2),
\end{aligned} \tag{32}$$

where $F_i^{W^+N_0}(x, Q^2) = \frac{1}{2}(F_i^{W^+p}(x, Q^2) + F_i^{W^+n}(x, Q^2))$. From above equations, we obtain the modified P-W relation with the asymmetry of $s(x)$ and $\bar{s}(x)$ considered:

$$R_N^- = \frac{\sigma_{NC}^{\nu N} - \sigma_{NC}^{\bar{\nu} N}}{\sigma_{CC}^{\nu N} - \sigma_{CC}^{\bar{\nu} N}} = R^- - \delta R_s^-, \tag{33}$$

where δR_s^- is the correction brought by the asymmetric distribution of strange-antistrange sea and R^- is the naive P-W relation with

$$\delta R_s^- = (1 - \frac{7}{3} \sin^2 \theta_w) \frac{S^-}{Q_V + 3S^-}, \tag{34}$$

and we define $Q_V \equiv \int_0^1 x[u_V(x) + d_V(x)]dx$ and $S^- \equiv \int_0^1 x(s(x) - \bar{s}(x))dx$. From above equations, we can find that the asymmetry of $s(x)$ and $\bar{s}(x)$ distributions should bring correction to $\sin^2 \theta_w$. The results are given in table II and III with the values of δR_s^- ranging from 0.00297 (0.00312) to 0.00826 (0.00867) corresponding to $\Lambda_K = \Lambda_\pi = 900 - 1500$ MeV for different inputting parameters. However, the $SU_f(3)$ symmetry breaking requires smaller $\langle P_K \rangle$ and $\langle P_\eta \rangle$ [52], so that we should adopt a smaller value for Λ_K such as from 900 MeV to 1100 MeV. Thus, the correction brought by the asymmetry of $s(x)$ and $\bar{s}(x)$ distributions should remove the NuTeV anomaly by about 60-100% within the effective chiral quark model. Although the magnitude of S^- with CQ model as input is almost twice larger than that with CTEQ parametrization as input, as pointed out in Sec. II, the calculated results of δR_s^- given in Table II and III are similar and not sensitive to the different inputs at fixed Λ_K . The reason may be that the uncertainties in the numerator and denominator of the Eq. (34) brought by the model can cancel out each other.

TABLE II: The results for CQ model input

Λ_k	Z	Q_v	S^-	δR_s^-
900	0.74888	0.86376	0.00558	0.00297
1000	0.73996	0.85484	0.007183	0.00384
1100	0.73063	0.84551	0.00879	0.00473
1200	0.72107	0.83595	0.01040	0.00562
1300	0.71143	0.82632	0.01198	0.00651
1400	0.70181	0.81669	0.01353	0.00740
1500	0.69227	0.80715	0.01503	0.00826

TABLE III: The results for CTEQ parametrization input

Λ_k	Z	Q_v	S^-	δR_s^-
900	0.74888	0.37089	0.00252	0.00312
1000	0.73996	0.36686	0.00322	0.00402
1100	0.73063	0.36247	0.00398	0.00498
1200	0.72107	0.35831	0.00468	0.00590
1300	0.71143	0.35395	0.00539	0.00683
1400	0.70181	0.34960	0.00612	0.00780
1500	0.69227	0.34528	0.00675	0.00867

IV. DISCUSSION ON ADDITIONAL SYMMETRIC SEA CONTRIBUTIONS

The asymmetries of light-flavor antiquark and strange-antistrange distributions originated from the nonperturbative sea have been discussed within the effective chiral quark model. Although the asymmetries of light-flavor antiquark and strange sea content in the nucleon are mainly coming from the intrinsic sea, the extrinsic sea should be also considered from a strict sense when we investigate the distributions of $\bar{d}(x) - \bar{u}(x)$, $\bar{d}(x)/\bar{u}(x)$ and $s(x)/\bar{s}(x)$. From the calculations, we find that the effective chiral quark model predictions of $\bar{d}(x) - \bar{u}(x)$ distributions keep consistence with the experimental data, but the predictions of $\bar{d}(x)/\bar{u}(x)$

distributions are not good in matching the experimental data at small and large x by using the effective chiral quark model before taking into account additional contribution from the symmetric sea (e.g. $\delta\bar{d}(x) = \delta\bar{u}(x)$). Because the contribution of the symmetric sea effect ($\delta\bar{d}(x) = \delta\bar{u}(x)$) cancels out each other in the distributions of $\bar{d}(x) - \bar{u}(x)$, the distributions of $\bar{d}(x) - \bar{u}(x)$ match the experimental data well. For the distributions of $\bar{d}(x)/\bar{u}(x)$, when the symmetric sea content is considered, the distribution of $\bar{d}(x)/\bar{u}(x)$ becomes:

$$\begin{aligned}\frac{\bar{d}(x)}{\bar{u}(x)} &= \frac{\bar{d}(x) + \delta\bar{d}(x) - \bar{u}(x) - \delta\bar{u}(x)}{\bar{u}(x) + \delta\bar{u}(x)} + 1 \\ &= \frac{\bar{d}(x) - \bar{u}(x)}{\bar{u}(x) + \delta\bar{u}(x)} + 1.\end{aligned}\tag{35}$$

From the Eq. (35), we can know that the ratio of $\bar{d}(x)/\bar{u}(x)$ will decrease if the symmetric sea is not zero. Here, we estimate the symmetric sea contribution $\delta\bar{u}(x) + \delta\bar{d}(x)$ ($\delta\bar{u}(x) = \delta\bar{d}(x)$) by the difference between the parametrization [53] of $\bar{u}(x) + \bar{d}(x)$ and the results predicted by effective chiral quark model. Thus, the distributions of $\bar{d}(x)/\bar{u}(x)$ without and with symmetric sea contribution are obtained and shown in Fig. 6. From the figure, we can find that a large suppression occurs by including the symmetric sea contribution, which implies that the effective chiral quark model only provides a fraction of the total light-flavor in the nucleon, and that a significant fraction of symmetric sea content is required. This also can be found in Fig. 7, which displays the comparison of the distributions for $\bar{u}(x)$ and $\bar{d}(x)$ obtained from the parametrization [53] and the effective chiral quark model calculations. The role of the symmetric sea is similar to that by including some isoscalar (pseudoscalar) meson σ (η) contribution in the meson cloud model, as pointed in Ref. [54]. However, the effective way of taking into account the symmetric sea contribution is not good in reproducing the shape of $\bar{d}(x)/\bar{u}(x)$, and more work both theoretically and experimentally should be done along this direction.

Within the effective chiral quark model, the strange-antistrange asymmetry mainly comes from the K meson clouds which accompany the constituent quarks. From the calculations we know that the corrections coming from the strange asymmetry with different inputs of constituent quark distributions are large enough to explain the NuTeV anomaly. It is also necessary to mention that the ratio of $s(x)/\bar{s}(x)$ in the model does not necessarily conflict with the experimental data in fact, because the experimental data include the effect of the intrinsic and extrinsic sea. In this paper, we calculate the ratio of $s(x)/\bar{s}(x)$ without and

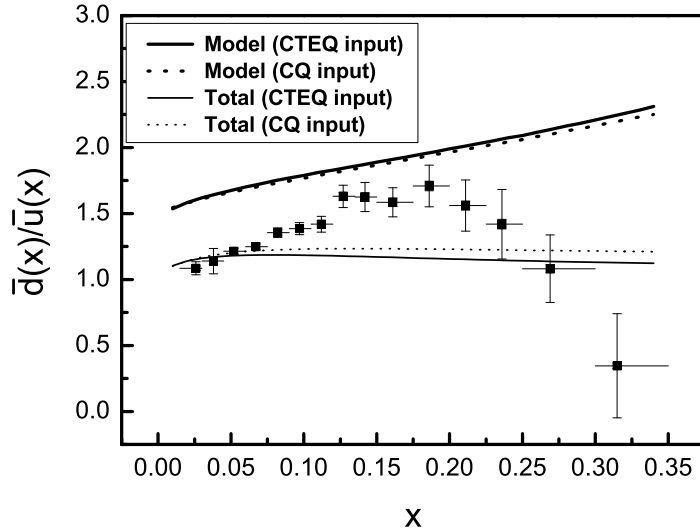


FIG. 6: The distributions of $\bar{d}(x)/\bar{u}(x)$ for $\Lambda_\pi = 1500$ MeV. The thick solid and dotted curves are the chiral quark model results with CTEQ6 parametrization and the CQ model as inputs. The thin curves are the corresponding results with both chiral quark model results and the symmetric sea contribution $\delta\bar{u}(x) = \delta\bar{d}(x)$ estimated by difference between the NuTeV data parametrization and the chiral quark model results. And the experimental data come from E866/NuSea ($Q^2 = 54$ GeV²) experiments [49].

with symmetric strange sea contribution, where the symmetric sea contribution is estimated effectively by the difference between $s(x) + \bar{s}(x)$ from the NuTeV data parametrization and that in the effective chiral quark model calculation, in similar to what we estimated above for the symmetric light-flavor sea quarks. The so called “NuTeV data parametrization” here is obtained by the NuTeV collaboration from the results of the leading order fits to the cross-section extracted from the NuTeV experimental data [50]. The strange sea parameterizations which break $\int_0^1 s(x)dx = \int_0^1 \bar{s}(x)dx$ as pointed out as in [14, 55] are defined conventionally by

$$\begin{aligned}
 s(x) &= \kappa \frac{\bar{u}(x) + \bar{d}(x)}{2} (1-x)^\alpha, \\
 \bar{s}(x) &= \bar{\kappa} \frac{\bar{u}(x) + \bar{d}(x)}{2} (1-x)^{\bar{\alpha}}.
 \end{aligned}
 \tag{36}$$

where the values of $\kappa, \bar{\kappa}, \alpha, \bar{\alpha}$ are taken from the NuTeV set of the Table III in Ref. [50]. And we give the comparison of $s(x)/\bar{s}(x)$ from the model prediction and that from the dimuon

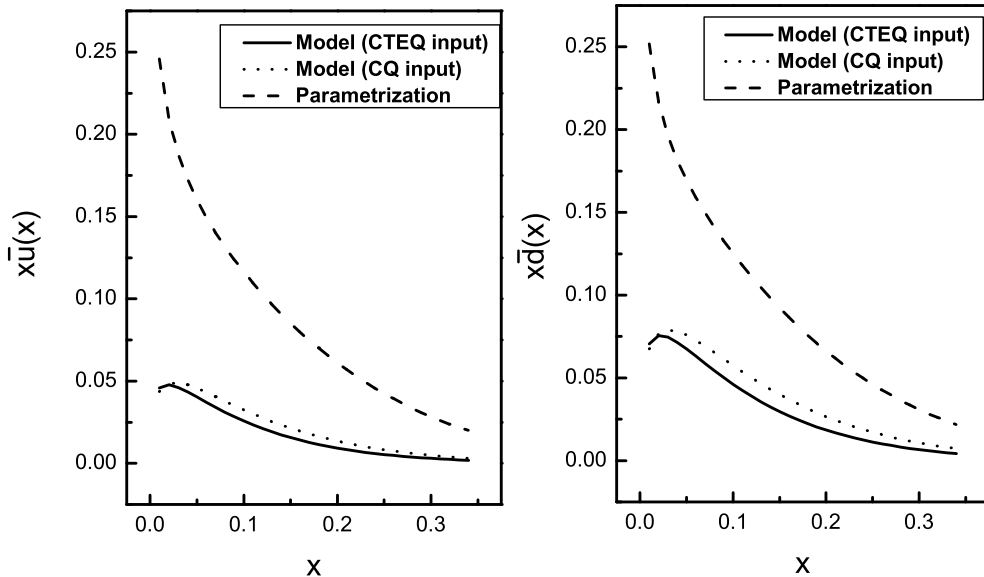


FIG. 7: The distributions of $\bar{d}(x)$ and $\bar{u}(x)$ for $\Lambda_\pi = 1500$ MeV. The solid and dotted curves are the effective chiral quark model results with CTEQ6 parametrization and CQ model inputs, and the dashed curve is for the NuTeV data parametrization.

measurements [50] in Fig. 8. From the left one of the figure without the symmetric sea content, we can see that the ratios are out of the area for errors. However, the distributions of $s(x)/\bar{s}(x)$ including the symmetric sea contribution are almost within the range of the experimental errors in the right one. This case is similar to the $\bar{d}(x)/\bar{u}(x)$ distribution and indicates that the effective chiral quark model only provides a fraction of the strange sea content, and that a significant fraction of symmetric strange sea content is still needed. Fortunately, the strange asymmetry of the effective chiral quark model can cause a large reduction of the NuTeV anomaly, although the asymmetric strange sea is only a small part of the total strange sea content of the nucleon.

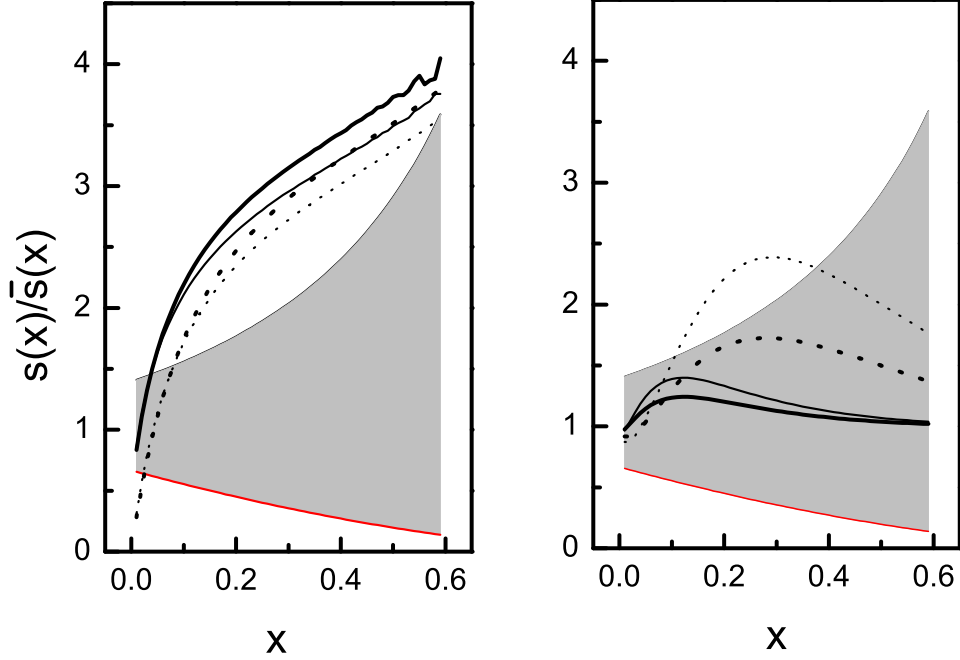


FIG. 8: Distributions of $s(x)/\bar{s}(x)$, where the shadowing area is the error range of NuTeV. The thick and thin solid curves are the effective chiral quark model results for $s(x)/\bar{s}(x)$ when $\Lambda_K = 900$ and 1100 MeV with CTEQ6 parametrization as input. The thick and thin dotted curves are the effective chiral quark model results for $s(x)/\bar{s}(x)$ when $\Lambda_K = 900$ and 1100 MeV with CQ model as input. The left side is the prediction by the effective chiral quark model only and the right side is the result by including both the prediction of the effective chiral quark model and the symmetric sea contribution estimated by the difference between the NuTeV data parametrization and the effective chiral quark model result.

V. SUMMARY

In this work, we presented the calculations of the asymmetries of light-flavor sea quark distributions $\bar{d}(x) - \bar{u}(x)$ and strange-antistrange $s(x) - \bar{s}(x)$ within the effective chiral quark model with more details along with our previous work [22] by using two different sets of parameterizations as inputs and find that the results for $\bar{d}(x) - \bar{u}(x)$ match the experimental measurements well. The distributions of $\bar{d}(x)/\bar{u}(x)$ do not match with the experimental data, but there is a large suppression of the ratio when the symmetric sea contribution

is considered. The contributions of symmetric sea effects are estimated effectively by the difference between the effective chiral quark model results and the data parametrization results. Fig. 4 and Fig. 7 indicate that the predictions of the effective chiral quark model provide only a fraction of the total light-flavor sea quarks and strange sea content of the nucleon. Also, we point out that the calculated results for $s(x)/\bar{s}(x)$ in the effective chiral quark model are consistent with the available experiments with an additional symmetric sea contribution being included effectively. More noticeably, the asymmetry of strange-antistrange distributions can bring a significant contribution to the NuTeV defect by at least 60% with reasonable parameters within this model, and the results are not sensitive to the different inputs of constituent quark distributions, although the intrinsic sea is not the dominant part in the nucleon sea. The effective chiral quark model is thus successful in explaining the nucleon sea anomalies not only about the GSR violation and the proton spin problem, but also about the NuTeV defect. Also, this may imply that the NuTeV anomaly can be considered as a phenomenological support to the strange-antistrange asymmetry of the nucleon sea. So it is more important that more precision experiments should be carried out to enable direct and more accurate determination of strange-antistrange sea quark distributions in the future.

VI. ACKNOWLEDGMENTS

This work is partially supported by National Natural Science Foundation of China (Nos. 10025523, 90103007, and 10421003), and by the Key Grant Project of Chinese Ministry of Education (No. 305001).

-
- [1] G.P. Zeller *et al.*, Phys. Rev. Lett. **88**, 091802 (2002).
 - [2] E.A. Paschos and L. Wolfenstein, Phys. Rev. D **7**, 91 (1973).
 - [3] E. Ma and D.P. Roy, Phys. Rev. D **65**, 075021 (2002); S. Davidson, *et al.*, JHEP **02**, 037 (2002); C. Giunti and M. Laveder, hep-ph/0202152; W. Loinaz *et al.*, Phys. Rev. D **67**, 073012 (2003); *ibid.* **70**, 113004 (2004); P. Langacker, J. Phys. G **29**, 1 (2003); A. Strumia, hep-ex/0304039; P. Gambino, Int. J. Mod. Phys. A **19**, 808 (2004).
 - [4] S. Kumano, Phys. Rev. D **66**, 111301(R) (2002).

- [5] M. Hirai, S. Kumano, and T.-H. Nagai, hep-ph/0412307.
- [6] S.A. Kulagin, Phys. Rev. D **67**, 091301(R) (2003).
- [7] S. Kovalenko, I. Schmidt, and J.-J. Yang, Phys. Lett. B **546**, 68 (2002).
- [8] G.A. Miller and A.W. Thomas, Int. J. Mod. Phys. A **20**, 95 (2005); G.P. Zeller *et al.*, hep-ex/0207052; S.J. Brodsky, I. Schmidt, and J.-J. Yang, Phys. Rev. D **70**, 116003 (2004); K.S. McFarland *et al.*, Nucl. Phys. Proc. Suppl. **112**, 226 (2002); J.-W. Qiu and I. Vitev, Phys. Lett. B **587**, 52 (2004).
- [9] B.-Q. Ma, Phys. Lett. B **274**, 111 (1992).
- [10] E. Sather, Phys. Lett. B **274**, 433 (1992).
- [11] J.T. Londergan and A.W. Thomas, Phys. Lett. B **558**, 132 (2003).
- [12] F.-G. Cao and A.I. Signal, Phys. Lett. B **559**, 229 (2003).
- [13] S. Catani, *et al.*, Phys. Rev. Lett. **93**, 152003 (2004).
- [14] S.J. Brodsky and B.-Q. Ma, Phys. Lett. B **381**, 317 (1996).
- [15] A.I. Signal and A.W. Thomas, Phys. Lett. B **191**, 205 (1987).
- [16] M. Burkardt and B.J. Warr, Phys. Rev. D **45**, 958 (1992).
- [17] H. Holtmann and A. Szczurek, J. Speth, Nucl. Phys. A **596**, 631 (1996).
- [18] Y. Ding and B.-Q. Ma, Phys. Lett. B **590**, 216 (2004). The “+” sign on the right side of eq.(7) before δR_g^- in this paper should be “-”.
- [19] J. Alwall and G. Ingelman, Phys. Rev. D **70**, 111505(R) (2004).
- [20] S. Kretzer *et al.*, Phys. Rev. Lett. **93**, 041802 (2004).
- [21] F. Olness *et al.*, Eur. Phys. J. C **40**, 145 (2005).
- [22] Y. Ding, R.-G. Xu, and B.-Q. Ma, Phys. Lett. B **607**, 101 (2005).
- [23] M. Wakamatsu, Phys. Rev. D **71**, 057504 (2005).
- [24] A. Szczurek, A.J. Buchmann, and A. Faessler, J. Phys. G: Nucl. Part. Phys. **22**, 1741 (1996).
- [25] K. Gottfried, Phys. Rev. Lett. **18**, 1174 (1967).
- [26] J. Magnin and H.R. Christiansen, Phys. Rev. D **61**, 054006 (2000).
- [27] F. Carvalho *et al.*, Eur. Phys. J. C **18**, 127 (2000).
- [28] R.D. Field and R.P. Feynman, Phys. Rev. D **15**, 2590 (1977).
- [29] J. Ashman *et al.*, Phys. Lett. B **206**, 364 (1988); Nucl. Phys. B **328**, 1 (1989).
- [30] S.J. Brodsky, J. Ellis, and M. Karliner, Phys. Lett. B **206**, 309 (1988); J. Ellis and M. Karliner, Phys. Lett. B **213**, 73 (1988); *ibid.* **341**, 397 (1995).

- [31] A.O. Bazarko *et al.* (CCFR Collab.), Z. Phys. C **65**, 189 (1995).
- [32] W.G. Seligman *et al.*, Phys. Rev. Lett. **79**, 1213 (1997); S.A. Rabinowitz *et al.*, Phys. Rev. Lett. **70**, 134 (1993).
- [33] M. Arneodo *et al.*, Nucl. Phys. B **483**, 3 (1997).
- [34] V. Barone, C. Pascaud, and F. Zomer, Eur. Phys. J. C **12**, 243 (2000).
- [35] P. Berge *et al.*, Z. Phys. C **49**, 187 (1991).
- [36] S. Weinberg, Physica A **96**, 327 (1979).
- [37] A. Manohar and H. Georgi, Nucl. Phys. B **234**, 189 (1984).
- [38] P. Amaudruz *et al.*, Phys. Rev. Lett. **66**, 2712 (1991); M. Arneodo *et al.*, Phys. Rev. D **50**, R1 (1994).
- [39] E.J. Eichten, I. Hinchliffe, and C. Quigg, Phys. Rev. D **45**, 2269 (1992).
- [40] T.P. Cheng and L.-F. Li, Phys. Rev. Lett. **74**, 2872 (1995).
- [41] K. Suzuki and W. Weise, Nucl. Phys. A **634**, 141 (1998).
- [42] S. Weinberg, Phys. Rev. Lett. **65**, 1181 (1990).
- [43] M. Glück, E. Reya, and M. Stratmann, Eur. Phys. J. C **2**, 159 (1998).
- [44] R.C. Hwa and M.S. Zahir, Phys. Rev. D **23**, 2539 (1981).
- [45] J. Pumplin *et al.*, JHEP **0207**, 012 (2002).
- [46] H.W. Kua, L.C. Kwek, and C.H. Oh, Phys. Rev. D **59**, 074025 (1999).
- [47] R.C. Hwa and C.B. Yang, Phys. Rev. C **66**, 025204 (2002); *ibid.* **66**, 025205 (2002).
- [48] K. Ackerstaff *et al.*, Phys. Rev. Lett. **81**, 5519 (1998).
- [49] R.S. Towell *et al.*, Phys. Rev. D **64**, 052002 (2001).
- [50] M. Goncharov *et al.*, Phys. Rev. D **64**, 112006 (2001).
- [51] J.T. Londergan and A.W. Thomas, Prog. Part. Nucl. Phys. **41**, 49 (1998).
- [52] X. Song, J.S. McCarthy, and H.J. Weber, Phys. Rev. D **55**, 2624 (1997).
- [53] H.L. Lai *et al.*, Phys. Rev. D **55**, 1280 (1997).
- [54] M. Alberg, E.M. Henley, and G.A. Miller, Phys. Lett.B **471**, 396 (2000); F. Huang, R.-G. Xu, and B.-Q. Ma, Phys. Lett. B **602**, 67 (2004).
- [55] D. Mason for the NuTeV Collaboration, hep-ex/0405037.